From phenotype to genotype in a Spanish CMT2P/*LRSAM1* family: a historical overview of follow-up over four decades

J. Berciano[1], A. Jordanova[2,3,4]

[1]Professor emeritus *ad honorem*. University of Cantabria. Former head of the Neurology Service at Marqués de Valdecilla University Hospital (IDIVAL) and researcher at Centro de Investigación Biomédica en Red de Enfermedades Neurodegenerativas (CIBERNED), Santander, Spain.
[2]Molecular Neurogenomic Group, VIB-UAntwerp Center for Molecular Neurology, University of Antwerp, Antwerp, Belgium.
[3]Department of Biochemical Sciences. University of Antwerp, Antwerp, Belgium.
[4]Department of Medical Chemistry and Biochemistry. Medical University of Sofia, Sofia, Bulgaria.

ABSTRACT

Objective. To perform a review of our long-term follow-up studies in a family with dominant inheritance of Charcot-Marie-Tooth disease type 2 (CMT2).

Development. The initial pedigree (1977-1985) comprised 10 affected individuals over three generations and 17 unaffected at-risk members. The clinical picture consisted of a mild peroneal muscular atrophy syndrome with incomplete penetrance in the first two decades of life. Histopathological study demonstrated that the underlying disease is a lumbosacral sensorimotor neuronopathy with length-dependent axonopathy. A tentative mapping of chromosome 12q12 (CMT2G) was performed in 2004. Subsequently, and continuing with serial clinical-electrophysiological examinations and MRI studies of calf and foot muscles, the clinical picture was redrawn, so that by 2016 there were 13 affected members. Starting from this modified pedigree, we redefined the disease-linked region to chromosome 9q and subsequently identified a novel missense variant of the E3 ubiquitin-protein ligase LRSAM1 (p.Cys694Tyr). This mutation does not influence overall protein levels of LRSAM1, nor its ubiquitylation target TSG101. The mutation is associated with several transcriptional changes, including significant upregulation of another E3 ubiquitin-protein ligase, NEDD4L, and of TNFRSF21, a key regulator of axonal degeneration.

Conclusions. The longitudinal study of this large CMT2 family with incomplete penetrance demonstrates its enormous value for a reliable phenotypic definition. This has made possible the identification of the causal genetic variant, which attests to the formidable and sustained coordination between Spanish clinicians and Belgian geneticists. Our findings demonstrate that the isolated genetic entity CMT2G is caused by a missense mutation in *LRSAM1* and should be reclassified as CMT2P.

KEYWORDS

Axonal degeneration, Charcot-Marie-Tooth disease type 2 (CMT2), CMT2G, CMT2P, electrophysiology, incomplete penetrance, LRSAM1, MRI, neuronopathy, next-generation sequencing, peroneal muscular atrophy, pes cavus, transcriptional changes

Introduction

Charcot-Marie-Tooth disease (CMT) is the most common inherited neuropathy with a prevalence rate in Cantabria of 28.2 cases per 100 000 population,[1] which is basically characterised by progressive wasting and weakness of distal muscles and pes cavus.[2-5] CMT was initially classified according to the mode of transmission (autosomal dominant, autosomal recessive, X-linked, or mitochondrial) and electrophysiological or nerve biopsy features. Characteristically, motor conduction velocities (MCV) in median nerve are < 38 m/s for the

Corresponding author: Dr José Berciano
E-mail: joseberciano51@hotmail.com

Received: 20 February 2025 / Accepted: 6 May 2025

demyelinating forms (CMT1) and > 38 m/s for the axonal form (CMT2).[2-5] There may be an intermediate form with MCV between 25 and 45 m/s.[6,7] CMT is a clinically and genetically complex disorder, with causal mutations in over 120 genes having been reported with the recent implementation of next-generation sequencing (NGS) into routine diagnostic practice.[8-10]

The main objective of this study is to provide an overview of a large Spanish CMT2 pedigree with autosomal dominant transmission followed up over four decades.[11-13] The precise genetic diagnosis, CMT2P/*LRSAM1*, would not have been possible without long-term follow-up of patients and at-risk subjects, given that the pedigree displayed very blatant incomplete penetrance. Narration and illustrations conform to our original descriptions and are presented in chronological study order.

Initial evaluation (1977-1986) of the AC pedigree: clinical-pathological study

Clinical features

Ten affected and 17 unaffected persons belonging to a single Cantabrian family, as shown in Figure 1, were evaluated by one of the authors (JB) from 1977 to 1985.[11] The disease in the pedigree was consistent with autosomal dominant inheritance. Seven of the 11 persons at risk in the third generation, with ages ranging from 22 to 41 years, were affected. By contrast, only one of the 10 persons at risk in the fourth generation, with ages ranging from one to 15 years, was affected; this proportion differs significantly from the expected ratio of 1:1 ($\chi^2 = 8.20$; $P < .01$).

The clinical features of the 10 affected members that had already been tabulated (see Table 1 in the paper by Berciano et al.[11]) will be updated and re-tabulated later in this work (see below). The ages of the 10 affected members of this family ranged between eight and 78 years, with a mean of 38 years. The majority developed symptoms during the second decade of life, with only two patients becoming symptomatic before or after that age. Two were asymptomatic, but presented subtle clinical signs. The main presenting symptoms were pes cavus (Figure 2) and difficulty walking. The affected members were at most only moderately disabled; in fact, no variation in neurological status was observed in successive examinations performed from 1977 to 1985. There was mild stocking hypoaesthesia, mainly involving vibratory sensitivity. Muscle weakness and amyotrophy were restricted to the small muscles of the feet and sometimes to leg muscles, especially the foot extensors; only one person showed the classical "stork legs" sign (Figure 2). There was lower-limb areflexia. Three patients (cases II-4, III-5 and III-7; see Figure 1[11]) have required orthopaedic surgery in their feet. Case III-5 sustained a comminuted fracture of the medial and lateral condyles of the right tibia in 1980, complicated by a painful plantar ulcer and osteomyelitis of metatarsal and tarsal bones. After a protracted clinical course, amputation of this leg was performed in February 1985 (see below for the histological study of leg nerves). Hand wasting, scoliosis, nerve thickening, pupillary anomalies, deafness, optic atrophy, tremor, and ataxia were not present. Results from routine laboratory tests and ECG were normal.

Case III-7 (propositus)

This 32-year-old man consulted in 1977 for progressive deformity of the right foot. He was a heavy smoker (more than 40 cigarettes per day). At the age of 17 years he had an operation for pes cavus. On examination at age 29, he showed bilateral pes cavus and distal wasting in the lower limbs, especially on the right side (Figure 3).[11,14] Tendon reflexes were absent in his legs and normal in his arms. He displayed mild stocking hypoaesthesia. The patient was re-examined in 1978 and 1979, and no changes were noted. In April 1980, he was admitted for subacute and progressive dyspnoea. Once again, neurological examination showed no changes. Chest radiography revealed a mass in the left lung. He died three weeks after admission. The general autopsy showed an oat cell carcinoma with metastases in regional lymph nodes, liver, spleen, adrenal glands and bone marrow.

Electrophysiological studies

The results of the electrophysiological studies will be presented in greater detail below, starting from follow-up examinations carried out between 2011 and 2015. Up to 1985, initial nerve conduction studies (motor and sensory) were performed on the median and peroneal nerves in all but two of the affected individuals. The results, tabulated in the paper by Berciano et al.,[11] can be summarised as follows: *i)* sensory nerve action potential (SNAP) amplitudes of the median nerve showed moderate reduction (22-58% of normal) in six adult subjects and were normal in two young patients; *ii)* two patients displayed minimal slowing of sensory conduction velocity (SCV); *iii)* SNAP of the peroneal nerve were examined in five

cases, being unobtainable in one case and showing reduced amplitude (33-66% of normal) in the remainder; *iv)* distal motor latencies (DML) were always normal in the median nerve, whereas they were slightly prolonged in the peroneal nerve; and *v)* MCVs were normal in the median nerve and slightly reduced in the peroneal nerve.

Electromyography of the tibialis anterior was performed in 10 affected individuals, revealing a chronic denervation pattern.

Between 1977 and 1985, the studies were repeated in seven cases, and no significant changes were observed.

Pathological studies

Pathological material included the following: *i)* autopsy of the proband patient (case III-7, Figure 1[11]); *ii)* dissection of the nerves of the amputated leg from case III-5, from which samples were taken of the deep peroneal (anterior tibial) and posterior tibial nerves in their upper, middle, and lower thirds, as well as from their distal branches (lateral terminal branch and medial plantar branch); and *iii)* sural nerves from cases III-5 and III-7.

At autopsy, the spinal cord and nerve roots were macroscopically normal. Figure 4A-F[11] illustrates the main findings from the spinal cord, nerve roots, and spinal ganglia. The grey matter of the anterior horn was normal at cervical and thoracic segments. Motor neuron cell loss (Figure 4A[11]) and gliosis were observed at the lumbosacral level; motor neurons frequently exhibited signs of neuronal atrophy, but neither central chromatolysis nor neuronophagia was observed. The four posterior root ganglia examined (L3-S1) displayed marked depletion of ganglion cell bodies, proliferation of satellite cells, and residual nodules of Nageotte (Figure 4C[11]). The L5 ventral and dorsal roots were studied, revealing loss of larger myelinated fibres, particularly in the dorsal root (Figure 4B, D[11]). Morphometric evaluation of spinal roots was only carried out at the L5 level (Supplementary Material figures S1a, b[11]). The proportion of large fibres (≥ 8 μm) in the ventral and dorsal roots was significantly lower than in controls ($P < .001$). There were clusters of small regenerating fibres (Figures 4B and 5A[11]); for quantification of cluster numbers, see Berciano et al.[11] Atrophic axons were occasionally encountered (Figure 5B[11]).

In the peripheral nerve trunks examined, the most striking pathological finding was a decrease in the number of myelinated fibres (Figure 6[11]). The diameter distribution histogram was unimodal in all nerves as a result of the disappearance of the largest myelinated fibres (Supplementary Material figures S1c, d[11]). A proximal-to-distal gradient of fibre loss was evident in peroneal and posterior tibial nerves. Clusters of regeneration were also observed (Figure 6[11]).

Definitive stage (1987-2015): phenotypic redefinition, molecular era entry, and pathogenic gene variant disclosure

In these three decades, a series of advances took place that that made it easier for us to better delineate the phenotype and identify a pathogenic variant of *LRSAM1*. As before, we will follow the chronological order of these events.

The collaboration between Dr Anita Harding and Dr José Berciano enters the scene

In 1983, Combarros et al.[15] had reported four CMT1 pedigrees comprising 47 examined individuals: 26 affected and 21 unaffected. Four years later, Dr Anita Harding (Institute of Neurology, Queen Square, London) requested our collaboration in her desire to perform linkage analysis in informative CMT1 pedigrees, and eventually in the AC family (CMT2) described here. The results of these CMT1 linkage studies were, successively, as follows: *i)* absence of linkage to chromosome 1 markers[16]; *ii)* confirmation of linkage to the pericentromeric region of chromosome 17[17]; and *iii)* confirmation of DNA duplication on 17p11.2 as a cause of CMT1A.[18] As might have been expected, two CMT2 pedigrees, including the AC family, did not show the CMT1A duplication.

From London to Antwerp

After the untimely death of Professor Anita Harding (in 1995, at the age of 43), DNA samples from the AC family were transferred to the Laboratory of Neurogenetics at the University of Antwerp, headed by Dr Christine van Broeckhoven; her laboratory was recognised as a leading centre after discovering that the basis of CMT1A was duplication in chromosome 17p11.2,[19] and after launching the European CMT Consortium. The fact is that over the course of the Seventh Meeting of the European Neurological Society, held in Rhodes (Greece) on 14-18 June, 1997, Dr van Broeckhoven contacted one the authors (JB) to confirm that DNA samples received from London belonged to the Spanish AC family, as was the

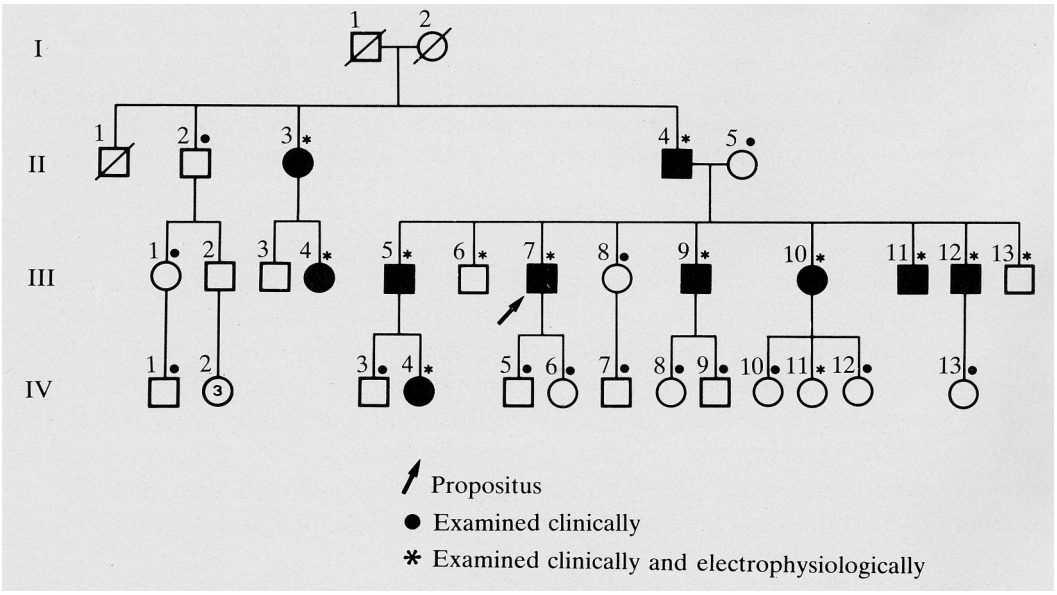

Figure 1. Pedigree of the AC family as reported by Berciano et al.[11]

Figure 2. Photographs of case III-5, obtained at age 34, showing peroneal muscle atrophy ("stork legs") (A). In the close-up images of the feet, note pes cavus with clawing of the toes and callosity on the anterior plantar arches (B, C). Note also the cutaneous scar sequelae of the surgical corrections for foot deformities (B). Unpublished images.

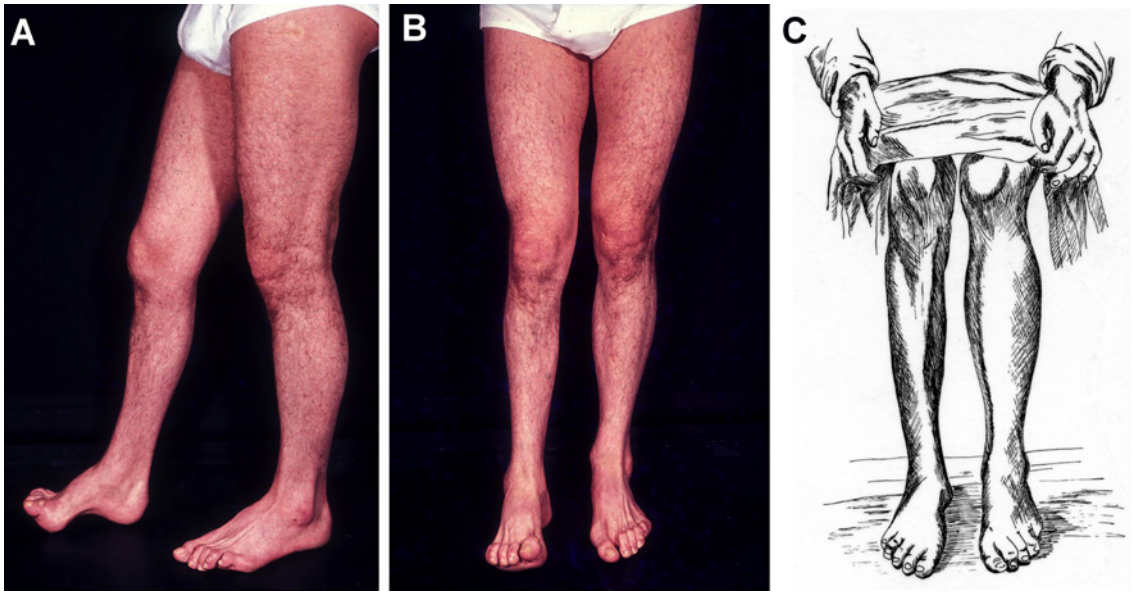

Figure 3. Propositus showing asymmetric peroneal muscular atrophy (A, B). There is a remarkable similarity with Case II by Tooth[14] (C, redrawn from the original). Taken from Berciano et al.[11]

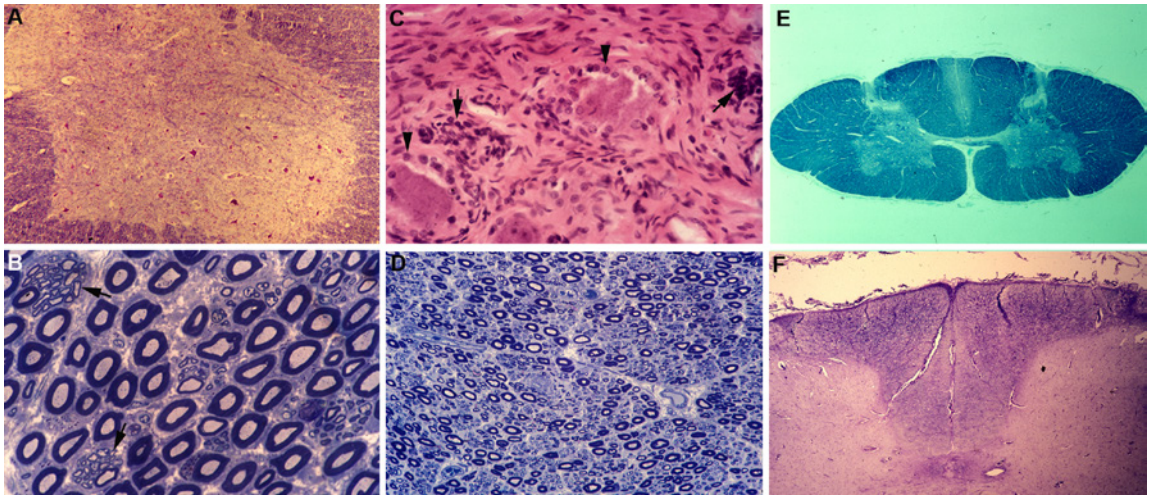

Figure 4. A) Transverse section of the spinal cord at the S1 segmental level, showing loss of motor cells in the anterior horn accompanied by gliosis (KB, original magnification ×250 before reduction. B) Semithin transverse section of the L5 ventral root showing two clusters of regenerating fibres (arrows); at this high power view, the loss of myelin fibres is not appreciable (Toluidine blue, original magnification ×1000 before reduction). C) Lumbar posterior root ganglion showing degenerated neuronal cell bodies with proliferation of capsule cells (arrowheads) and residual nodules of Nageotte (arrows) (HE, original magnification ×400 before reduction). D) Semithin section of the L5 dorsal root, showing reduction of larger myelinated fibres, the smaller one being increased (Toluidine blue, original magnification ×400 before reduction). For fibre histograms of myelinated fibres of L5 roots, see Supplementary Material figure S1a. E) Transverse section of the spinal cord at the C5 level, showing bilateral demyelination of fasciculus gracilis (KB, original magnification ×25 before reduction). F) Transverse section of the spinal cord at the S1 level, showing marked gliosis of posterior columns (Holzer, ×100 before reduction). Adapted from Berciano et al.[11]

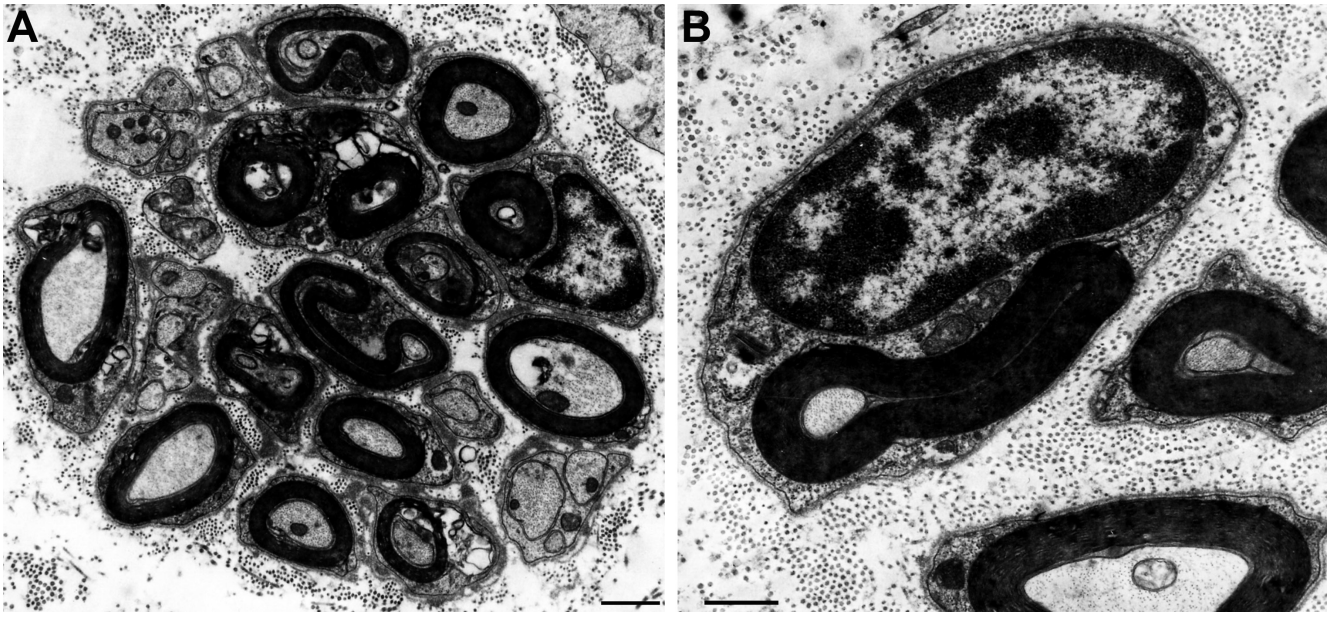

Figure 5. Electron micrographs of the L5 ventral root. A) Cluster of regenerating fibres containing myelinated and non-myelinated axons. B) Attenuated axon in a myelinated fibre. (Bars = 1 μm). Taken from Berciano et al.[11]

case because the family tree was the one hand-drawn by JB when the first shipment was made from Santander to London in 1987. On our return to Santander, JB sent Dr van Broeckhoven a copy of the clinical and pathological material published on this family.[11] JB made a commitment to conduct a clinical update of the patients and subjects at risk in the following months.

By 2002, the AC pedigree was clinically updated with the addition of one new affected member in the third generation (case III-20) and four additional cases in the fourth generation (cases IV-5, IV-9, IV-10, and IV-11) (Supplementary Material figure S2[12,13]). Based on the updated pedigree, Nelis et al.[12] carried out a genome-wide linkage analysis. A conclusive linkage with the chromosome 12q13.13 marker was obtained. Fine mapping localised this novel locus to a 13.2-Mb (12.8 cM) interval between D12S1663 and D12S1644 at 12q12-q13.3. The candidate genes *AVIL*, *CENTG1*, *RAB5B*, and *DHH* were excluded. It was concluded that the CMT2 neuropathy in this family represented a novel genetic entity, designated CMT2G.

Consecutive clinical studies in Santander and molecular genetic research in Antwerp continued in parallel

In the following years, a series of advances took place, which can be summarised as follows:

— Introduction of the CMT neuropathy score (CMTNS), which, using clinical and electrophysiological parameters, provides a single measure to quantify CMT disability.[20] CMTNS can vary between 0 and 36, and CMT is classified as mild (scores ≤ 10), moderate (11-20) and severe (≥ 21). It is worth noting that the CMTNS is a validated measure of length-dependent axonal and demyelinating CMT disability and can be calculated as an end point for longitudinal studies and clinical trials in CMT.[20,21]

— Pes cavus is a cardinal manifestation of CMT.[2-5,22-26] On the basis of our longitudinal electrophysiological studies in children with CMT1A, we postulated that forefoot cavus is initiated by denervation of the intrinsic foot muscles, and particularly the lumbricals.[23-25] This pathophysiological proposal was subsequently confirmed by MRI examination of the leg and foot muscles

in CMT1A patients. In patients with mild CMTNS, fatty muscle atrophy predominantly or exclusively involved the intrinsic foot muscles.[27]

— With its commercial introduction in 2005, NGS greatly facilitated genetic diagnosis in CMT.[8,28] NGS technology allows high-throughput parallel sequencing either of targeted genes (panels), all protein-coding sequences (whole exome sequencing [WES]), or the entire genome (whole genome sequencing [WGS]).

Gene hunting within the AC pedigree

In 2010, Guernsey et al.[29] studied a large autosomal recessive CMT2 pedigree, in which they found homozygosity for a splice mutation in the leucine-rich repeat- and sterile alpha motif-containing 1 (*LRSAM1*) gene, located at chromosome 9q33.3-q34.1 (OMIM # 614436); heterozygous mutation carriers were unaffected. Soon after, at the VIB Department of Molecular Genetics (Antwerp), extensive molecular genetic and genomic studies were carried out on the AC family; these have been described in detail elsewhere by Peeters et al.[13] In brief, the analyses performed are as follows: array comparative genomic hybridisation targeting the CMT2G locus, linkage analysis, new whole-genome linkage analysis, and WGS/WES of cases II-2 and III-1 (Figure 7A[11-13]); nevertheless, no disease-causing mutation could be found within the chromosome 12q12-q13-3 locus. This molecular finding forced us to update, between 2011 and 2025, the clinical, electrophysiological, and imaging data, and to reassess molecular features in at-risk subjects, whether they were symptomatic or only showed clinical signs of peroneal muscular atrophy.

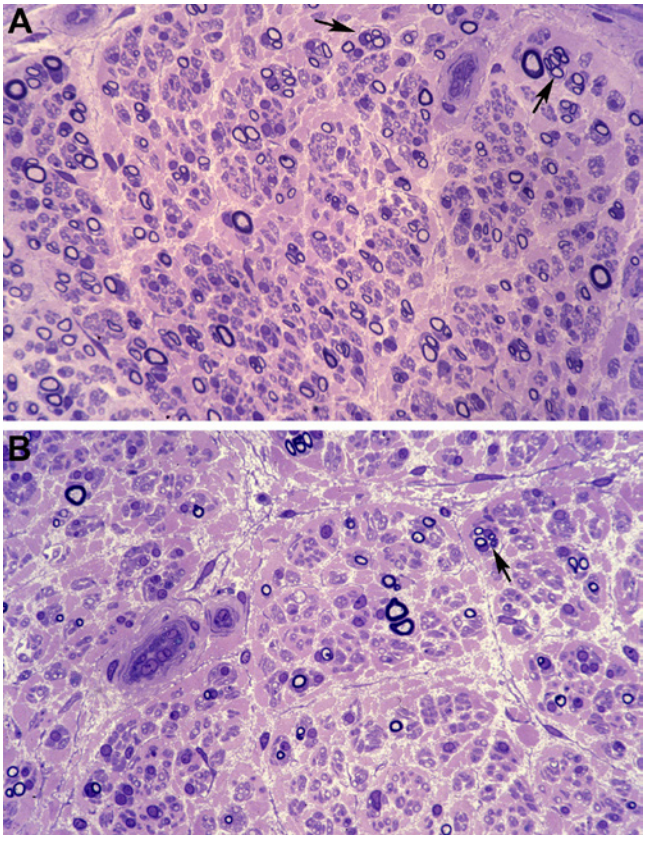

Figure 6. These images illustrate the pathological hallmark of the posterior tibial nerve in Case III-5 (see text for further details). Semithin transverse sections of the upper third (A) and the lower third (B) of the nerve, showing loss of myelinated fibres, with an evident proximal-to-distal gradient in this fibre loss; note that the density of myelinated fibres is far lower than that seen in the lumbar roots (see Figure 4). Several fibres contain thin myelinated sheaths in relation to axon diameter, a feature suggestive of remyelination. Note also clusters of regeneration (arrows) (Toluidine blue, ×250 before reduction). Adapted from Berciano et al.[11]

Clinical findings

Firstly, it should be noted that cases II-1, II-2 and their descendants and descendants of case II-3 were excluded from the updated pedigree (compare Figures 1 and 7A).[11,13] To avoid interpretative errors in the genealogy of this family, when mentioning specific cases we will refer to figures with genealogical representation (Figures 1 and 7,[11,13] or Supplementary Material figure S2[12,13]). Updated clinical data from the latest examinations, performed between 2011 and 2015 in all 11 affected subjects, are summarised in Table 1[13]; this allowed the identification of new cases in the fourth generation (cases IV-1, IV-10, and IV-2), but also the exclusion of previous cases considered affected (III-12, III-14, IV-8, and IV-9) (compare the pedigrees in Figure 7A[11-13] and Supplementary Material figure S2[12,13]). Four patients (II-1, II-2, III-1, and III-4 in Figure 7A[11-13]) died from causes unrelated to CMT; none of them had exhibited progression of lower-limb weakness. Both re-examined patients from the third generation (III-8 and III-10) showed progressive walking difficulties requiring neither ankle/foot orthosis nor support; CMTNS was mild or moderate (Table 1[13]). All affected members of the fourth generation have remained asymptomatic with mild CMTNS. Two patients (cases IV-4 and IV-11 in Figure 7A[11-13]) showed pes cavus, stocking hypoaesthesia, and lower-limb areflexia. Non-symptomatic

progression of lower-limb amyotrophy was observed in patient IV-4 (Figure 8A-D[13]). Figure 8E-I[13] shows patient IV-11 exhibiting minimal clinical involvement, consisting of forefoot cavus, toe clawing, stocking hypoaesthesia, and ankle areflexia. The remaining patients from the fourth generation presented only isolated pes cavus or no sign of disease.

Our longitudinal clinical evaluations revealed changes in some disease statuses compared to previous reports.[11,12] Case III-12 (Figure 7A[11-13]) is a 57-year-old man displaying pes cavus and minimal stocking hypoaesthesia. At age 26 years, the only positive electrophysiological finding had been reduced SNAP amplitude in peroneal nerves (0.5 μV; normal range, ≥ 1.5); he was considered affected (case III-16 in Supplementary Material figure 2).[11-13] Serial examinations (the latest was performed in 2014) revealed no signs of disease except for minimal pes cavus. Furthermore, the results of a follow-up electrophysiological study, including peroneal nerve motor and sensory parameters, were normal. Therefore, we reclassified him as unaffected. Case III-14 (Figure 7A[11-13]) is a 53-year-old man initially evaluated at the age of 13 years, when he presented only mild pes cavus and doubtful stocking hypoaesthesia with preserved tendon reflexes and muscle strength of the foot dorsiflexors/evertors. In our 2004 report,[12] he was considered affected (case III-20 in Supplementary material figure S2[12,13]). Nerve conductions were normal. Serial examinations over 20 years revealed no changes; therefore, he has been reassigned as unaffected.

Two other cases deserve special mention: sister and brother, cases IV-8 (born in 1976) and IV-9 (born in 1979) are listed as unaffected in the original pedigree (Figure 1)[11] and as affected in the pedigree by Nelis et al.[12] (Supplementary Material figure S2; cases IV-9 and IV-10[12,13]). Case IV-8 was found to be normal at the first examination at six years of age, whereas in subsequent consecutive examinations, between 1986 and 2000, pes cavus was observed, although nerve condition study findings were normal. In 2011 (at 35 years of age) and except for minimal pes cavus, clinical examination findings were normal, as were the results of nerve conduction studies and MRI of the lower-leg and foot muscles (see below). Therefore, she is now considered unaffected (Figure 7[11-13]; case IV-8). Case IV-9 (Figures 1 and 7A[11,13]) was aged 35 years in 2014. From the initial evaluation he had presented only mild pes cavus and incipient toe clawing; in 2002 he was considered presumably affected (case IV-10 in Supplementary Material figure S2[12,13]). Repeated examination in 2014 revealed no difficulty in heel walking, with normal ankle flexor-extensor muscle strength. Ankle and patellar reflexes were preserved. Nerve conduction study results were normal. It is worth noting that he was a professional football player. Given this minimal semiology and the absence of progression over two decades of observation, we concluded that this subject was not affected.

Electrophysiological findings

Electrophysiological studies were updated for eight affected individuals (Table 2; cases identified as numbered in Figure 7A).[11-13] Besides isolated SNAP amplitude reduction of the median nerve, potentially associated with an incidental carpal tunnel syndrome, two patients (IV-1 and IV-12) had normal nerve conduction studies, furthermore, needle electromyography (tibialis anterior and extensor digitorum brevis [EDB] in IV-1; EDB in IV-12) revealed no changes. In the remaining six patients, the most common finding was variable SNAP amplitude reduction in the median, ulnar, or sural nerve. Compound muscle action potentials (CMAP) in the ulnar and median nerves were systematically preserved, whereas in the tibial and/or peroneal nerves they were attenuated in four cases. MCVs and SCVs were normal or slowed in the axonal range; likewise DMLs were normal or slightly prolonged. Electromyography of the EDB systematically revealed a pattern of chronic denervation.

MRI findings

MRI of the lower-limb muscles was performed in eight individuals: two symptomatic patients (III-8 and III-10) and six at risk (IV-1, IV-4, IV-8, IV-10, IV-11, and IV-12) (numbering according to Figure 7A).[11-13] Only in case IV-8, not carrying the disease-causing mutation (see below), lower-leg and foot muscles were preserved (Figure 9A-C[13]). However, in the other seven (all mutation carriers), MRI revealed changes that became more evident with disease progression (see Figure 9D-I[13]). Calf muscles showed fatty atrophy, which was bilateral, at most moderate, predominantly distal, and mainly involved superficial posterior compartments. Calf muscle oedema was exceptional. Contrast enhancement, studied in cases III-8 and III-10, was not observed. Compared to the lower-leg muscles, the intrinsic muscles of the foot systematically exhibited more advanced fatty atrophy (Figures 9F and I[13]).

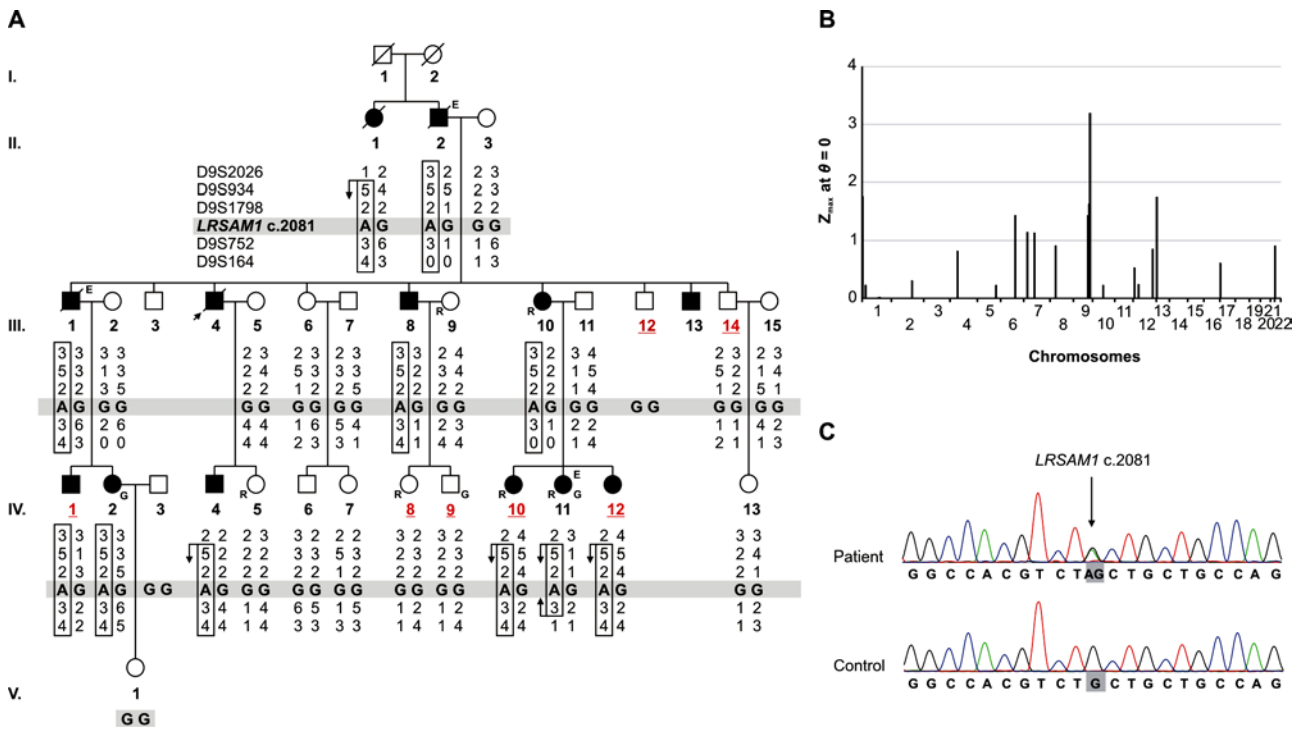

Figure 7. A) Updated pedigree and haplotype analysis of the Spanish AC pedigree in 2015. Note that in order to facilitate the reading of the at-risk subjects undergoing molecular study, the structure of the family tree has been modified with respect to the pedigrees given in the initial clinical-pathological study[11] (see Figure 1) and in the description of CMT2G[12] (see Supplementary Material figure S2[12,13]). Square symbols represent males and circles represent females. Black symbols indicate affected individuals. Underlined labels specify the individuals whose disease status was changed after clinical re-evaluation. Individuals who were subjected to whole genome, whole exome, or RNA sequencing are indicated with G, E, and R, respectively. Haplotype analysis indicates a disease-linked haplotype on chromosome 9. B) Graph representing the results of the genome-wide two-point parametric linkage analysis. Note that the initial linkage peak corresponding to CMT2G on chromosome 12 disappeared, whereas a new conclusive linkage region appeared on chromosome 9q31.3-q34.2 (Z_{max} = 3.186 at θ = 0). C) Electropherograms around the LRSAM1 c.2081 genomic position demonstrating a heterozygous G>A transition in a patient compared to a control. Taken from Peeters et al.[13]

Genetic findings: linkage studies

We recruited additional family members (cases IV-1, IV-5, IV-10, IV-12, and IV-13; Figure 7A[11-13]) and considered the updated disease status of seven individuals (see above).[13] Owing to the minimal clinical phenotype in the fourth generation, the disease status of four asymptomatic individuals (IV-5, IV-8, IV-9, and IV-12) was deemed "unknown." The renewed genome-wide linkage analysis demonstrated that the CMT2G region on chromosome 12q12-q13.3 was no longer linked to the disease phenotype[12]; however, a new conclusive linkage region appeared on chromosome 13q31.3-q34.2 (Z_{max} = 3.186 at θ = 0; Figure 7B[11-13]). Genotype analysis confirmed a common haplotype shared by all affected individuals (see Figure 7B[11-13]). Key recombination events (in II-1, IV-4, IV-10, IV-11, and IV-12) delineated the disease haplotype to a 23.6-Mb region between markers D9S2026 and D9S164.

Genetic findings: mutation analysis

We re-analysed the WGS data to find novel coding variants in the chromosome 9 locus, shared between the affected individuals (IV-2 and IV-11; Figure 7A[11-13]) and absent from the unaffected individual (IV-9).[13] Data filtering revealed no such variant; therefore, to exclude false-negative calls, we additionally analysed WES data from three affected individuals (II-2, III-1, and IV-11). WES analysis revealed a shared novel missense variant (c.2081G>A, p.Cys694Tyr; Figure 7C[11-13]) in the

Table 1. Clinical features of screened *LRSAM1* mutation carriers. Taken from Peeters et al.[13]

Case	Age (years)	Age at onset (decade)	Distal weakness in the LL	Areflexia			Sensory changes		Pes cavus	CMTNS
				UL	KJ	AJ	UL	LL		
II-1	84*	5	+	–	–	+	–	+	+	6**
II-2	85*	2	+	–	+	+	–	+	+	9**
III-1	58*	2	+	+	+	+	+	+	+	11**
III-8	64	2	+	–	–	+	+	+	+	7
III-10	59	2	+	+	+	+	+	+	+	9
IV-1	47	A	–	–	–	–	–	–	+	3
IV-2	41	A	–	–	–	–	–	–	+	0
IV-4	44	A	–	–	+	+	–	+	+	5
IV-10	40	A	–	–	–	–	–	–	+	3
IV-11	38	A	–	–	–	+	–	+	+	3
IV-12	35	A	–	–	–	–	–	–	–	0

A: asymptomatic; AJ: ankle jerk; CMTNS: Charcot-Marie-Tooth disease neuropathy score; KJ: knee jerk; LL: lower limbs; UL: upper limbs.

*: age at death; **: CMTNS retrospectively estimated11; +: presence of abnormality; –: absence of abnormality.

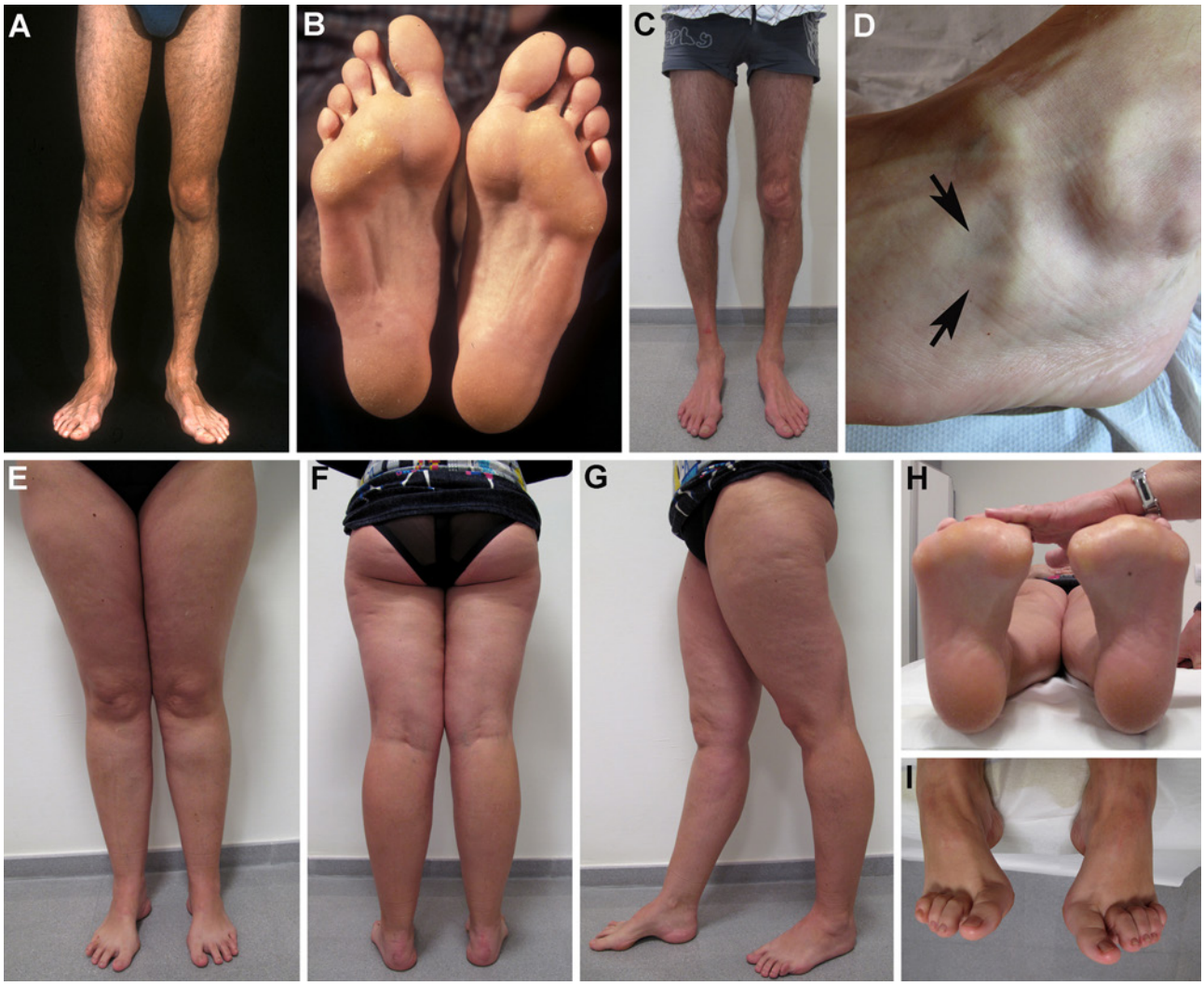

Figure 8. Updated clinical findings. Serial pictures of Case IV-4 (A-D), and pictures of Case IV-11 (E-I) taken at age 32 years (for number identification, see Figure 7). A) At age 25, the lower limbs appear normal; in particular, note the absence of peroneal muscular atrophy and toe clawing. B) Close-up picture of the soles of the feet, showing midfoot hollowing and callosity over transverse arcus plantaris and external foot borders. C) At age 43, note the appearance of lower leg amyotrophy, mainly involving peroneal muscles; in spite of this, there was evidence of neither weakness of foot extensors/evertors nor difficulty in heel walking. D) Close-up picture of the left foot, showing wasting of the extensor digitorum brevis muscle (arrows). E-G) There is no evidence of lower leg amyotrophy; note that even under load, pes cavus and clawing of toes are visible (E, G). H-I) Close-up pictures of the feet, showing marked pes cavus-varus deformity and toe clawing. Taken from Peeters et al.[13]

Table 2. Electrophysiological features (for patient numbering see Figure 7). Taken from Peeters et al.[13]

	III-8	III-10	IV-1	IV-2	IV-4	IV-10	IV-11	IV-12	Normal
Median nerve									
DML (ms)	4.0	3.8	3.1	3.4	2.9	**4.6**	3.6	2.5	≤ 4.4
MCV (m/s)	56.2	49.0	58.6	55.4	59.1	52.9	53.0	62.5	≥ 49.0
CMAP (mV)	6.3	5.6	9.7	4.7	6.9	4.8	7.6	10.1	≥ 4.0
F wave (ms)	30.4	**33.2**	28.0	25.7	24.3	30.6	30.8	25.3	≤ 31.0
SCV (m/s)	48.5	**42.3**	50.0	48.4	50.8	**37.9**	52.0	57.1	≥ 45.0
SNAP (μV)	**1.9**	**2.1**	**2.4**	9.8	**3.9**	**0.37**	**2.9**	8.4	≥ 7.0
Ulnar nerve									
DML (ms)	NS	2.6	2.4	NS	2.4	2.9	2.4	2.1	≤ 3.3
MCV (m/s)	NS	**42.3**	53.8	NS	61.7	54.3	57.1	63.9	≥ 49.0
CMAP (mV)	NS	**3.7**	7.0	NS	7.8	11.0	10.9	7.7	≥ 6.0
F wave (ms)	NS	**36.1**	32.4	NS	26.5	27.6	29.1	26.0	≤ 32.0
SCV (m/s)	NS	48.1	53.2	NS	53.1	47.7	56.0	54.2	≥ 47.0
SNAP (μV)	NS	**0.5**	3.0	NS	**1.6**	3.9	5.5	3.0	≥ 3.0
Peroneal nerve									
DML (ms)	**6.2**	5.1	5.5	**5.6**	5.5	**5.6**	4.2	3.9	≤ 5.5
MCV (m/s)	**39.9**	**33.5**	46.4	51.2	**41.1**	46.1	44.3	51.9	≥ 44.0
EDB CMAP (mV)	4.7	**0.7**	3.3	2.6	**1.8**	**1.3**	3.0	6.6	≥ 2.0
TA CMAP (mV)	NS	**3.3**	7.3	NS	7.6	5.1	6.2	5.4	≥ 5.0
F wave (ms)	55.4	A	53.8	49	A	51.7	48	46.7	≤ 56.0
Tibial nerve									
DML (ms)	**5.9**	A	5.8	5.1	4.8	4.0	**6.1**	NS	≤ 5.8
MCV (m/s)	43.0	A	43.7	48.1	**36.3**	49.2	41.1	NS	≥ 41.0
CMAP (mV)	**2.9**	A	5.5	12.5	4.4	9.1	4.8	NS	≥ 4.0
F wave (ms)	**57.6**	A	52.6	NS	53.5	51.4	**57.4**	NS	≤ 56.0
Sural nerve									
SCV (m/s)	47.3	A	49.1	**36**	44.8	52.9	46.7	53.1	≥ 40.0
SNAP (μV)	**4.1**	A	6.3	**0.6**	7	**2.9**	**1.3**	8.1	≥ 6.0

A: absent; CMAP: compound muscle action potential; DML: distal motor latency; EDB: *extensor digitorum brevis* muscle; MCV: motor conduction velocity; NS: not studied; SCV: sensory conduction velocity; SNAP: sensory nerve action potential; TA: tibialis anterior muscle. Abnormal values are indicated in bold.

LRSAM1 gene. This gene has already been associated with CMT2P.[29-32] This particular genomic position was not covered in the WGS data of the two affected individuals. The *LRSAM1* variant was present in all disease haplotype carriers and absent from 164 Spanish control individuals. It targets a conservative nucleotide (Genomic Evolutionary Rate Profiling score = 5.26) and amino acid residue (PolyPhen2 score = 0.998) within the catalytic RING-type zinc finger domain of the LRSAM1 protein.

Protein studies

Reported *LRSAM1* pathogenic variants affect the length[30-32] or abundance[29] of the protein. Therefore, we compared LRSAM1 protein levels in lymphoblasts from five mutation carriers and four non–mutation carriers, yet observed no difference in expression between both groups (Figure 10A).[13] Additionally, a reported *LRSAM1* mutation affecting the RING domain disturbs its ubiquitin ligase activity, resulting in increased abundance of its ubiquitylation target TSG101.[30,33] We tested a potential effect of the mutant protein on TSG101, but comparable expression was detected in patients and controls (Figure 10A[13]).

Transcriptional analysis

Differential expression analysis of the lymphoblast transcriptome of three *LRSAM1* mutation carriers (III-10, IV-10, and IV-11; Figure 7[11-13]) compared three non-carriers (III-9, IV-5, and IV-8) revealed several misregulated transcripts (Figure 10B[13]; Supplementary Material table S1).[13] With reverse transcription quantitative PCR, we validated 35 protein-coding genes that showed a significant expression change (log-transformed fold-change ≥ 0.5 with both DESeq2 and edgeR algorithms, and ≥ 100 raw read counts in all samples of at least one group [Supplementary Material table S1][13]). To expand the relevance of our findings, we added samples of two more mutation carriers (III-8, IV-12) and one non-carrier (IV-9). We identified six significantly upregulated and two downregulated transcripts in patients' lymphoblasts (see Figure 10C[13]), including *NEDD4L*, another ubiquitin E3 ligase, and *TNFRSF21*, a key regulator of axonal degeneration.

Discussion

We describe here a longitudinal study conducted over four decades in a large CMT2 family. At the initial evaluations, carried out between 1977 and 1985, there were 10 examined patients of both sexes in three generations with male-to-male transmission, which is indicative of an autosomal dominant inheritance pattern.[11] The disease manifests with a mild-to-moderate neuropathy phenotype consisting of pes cavus, slight stocking hypoaesthesia and peroneal amyotrophy with little clinical progression. Asymmetric peroneal amyotrophy, as described by Tooth,[14] was exclusively observed in our proband patient (Figure 311,14); strikingly, up to 9.4% of CMT1A patients show asymmetrical lower-limb strength.[34] Seven of the 11 persons at risk in the third generation, with ages ranging from 22 to 41 years, were affected; conversely, only one of the 10 persons at risk in the fourth generation, with ages ranging from one to 15 years, was affected. This suggests incomplete penetrance in the first two decades of life, a genetic feature that has rarely been described in CMT. [30,31,35]

Our pathological study demonstrated a lumbosacral sensorimotor neuronopathy with length-dependent axonal degeneration (dying-back phenomenon).[11] This is a unique pathological study, since it combines examination of the spinal cord with a morphological and morphometric analysis of the L5 anterior and posterior roots, and lower-leg nerves (peroneal and posterior tibial nerves), comparing the findings from proximal and distal nerve segments. Pathological study also included the sural nerve in two cases, with similar findings to those observed in other lower-leg nerves.

In 1983 the research group of one the authors (JB) reported four extensive CMT1 families,[15] and shortly thereafter the current CMT2 pedigree.[11] This attracted the attention of Dr Anita Harding (National Hospital, Queen Square, London), who was at that time interested in mapping possible pathogenic genes, by linkage analysis, from families with three or more patients and as many at-risk unaffected subjects as possible. And so began an active collaboration that involved sending clinical data and blood samples to her for DNA extraction, which resulted in confirmation of CMT1A linkage to the pericentromeric region of chromosome 17,[17] and confirmation that DNA duplication on 17p11.2 was a cause of CMT1A (see above).[18] It is worth noting that two out of the eight CMT1A duplication families had been originally reported as showing linkage to the Duffy blood group on chromosome 1.[36] However, the AC family remained without a molecular diagnosis; it is worth noting that none of the patients in this pedigree exhibited signs

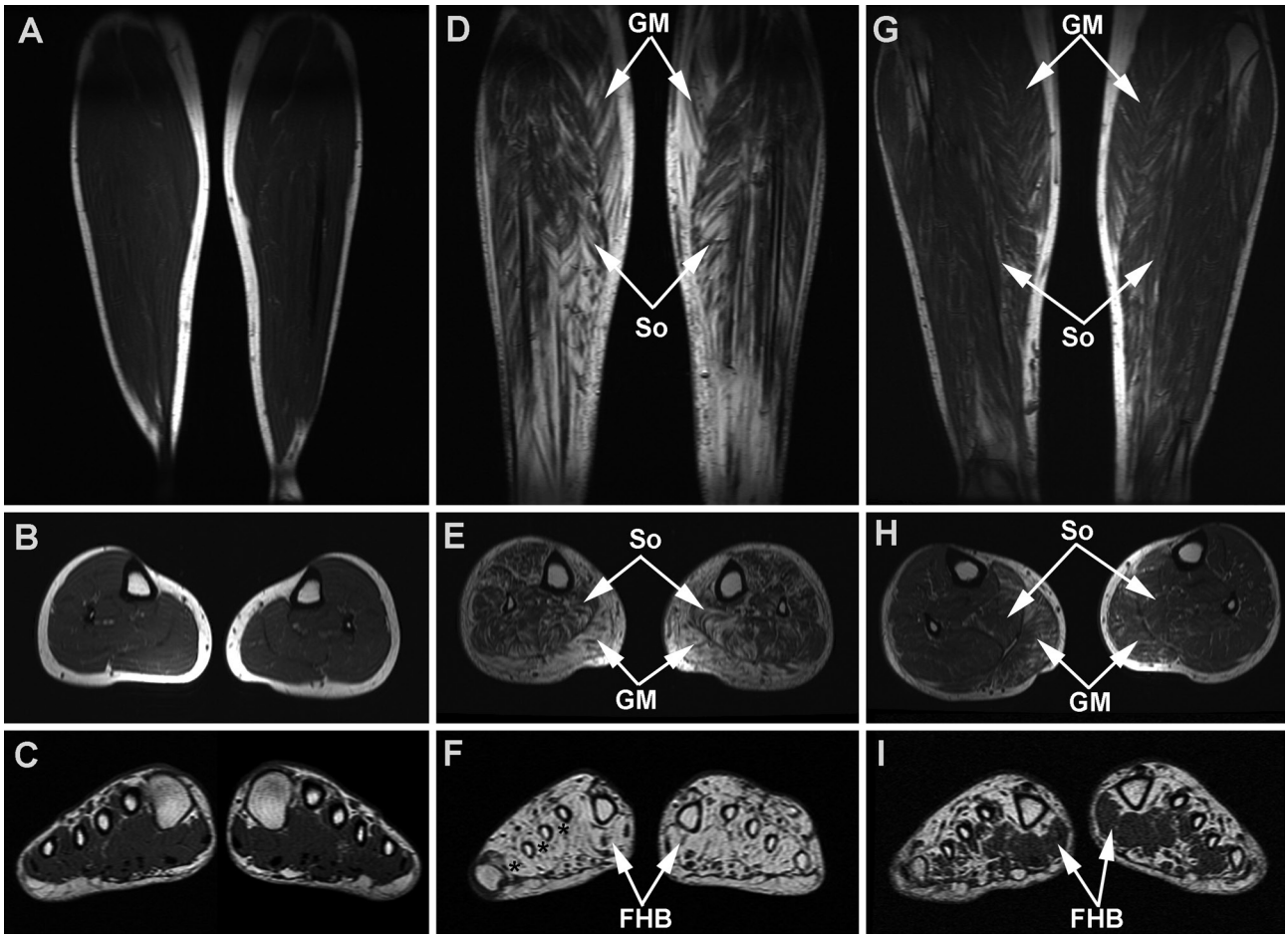

Figure 9. MRI study of the lower-limb muscles. T1-weighted MR images of the lower legs in the coronal plane thorough posterior aspect (top row) and the axial plane at the mid-calves (middle row), and of the feet through the metatarsal bones (bottom row). A-C) In Case IV-8 (see Figure 7), aged 38 years showing normal physical examination findings and no *LRSAM1* mutation, note preservation of the calf and foot muscles. D-F) In Patient III-10 (see also Figure 7), note predominantly distal fatty infiltration of all four muscle compartments, mainly involving the soleus (So) and gastrocnemius medialis (GM) muscles; there is massive fatty atrophy of the intrinsic foot muscles, with the right interossei (asterisks) and flexus hallucis brevis (FHB) being indicated. G-I) In patient IV-1, note mild and predominantly distal fatty infiltration of the soleus (So) and gastrocnemius medialis (GM) muscles; atrophy of the intrinsic foot muscles is more advanced, with the FHB being indicated. Taken from Peeters et al.[13]

characteristic of CMT1A, such as nerve enlargement or nerve conduction slowing in the demyelinating range.

As fate would have it (see above), AC family clinical data and DNA samples were transferred from the Mothercare Department of Paediatric Genetics (London, UK) to the Molecular Genetics Department (Antwerp, Belgium) in 1996. Following scientific contact between Dr Christine Van Broeckhoven and Dr José Berciano at the Seventh Meeting of the European Neurological Society (Rhodes, 1997), they decided to carry out linkage analysis on this large family; this required re-evaluation of the 10 subjects at risk in the fourth generation, since only one of them had been found to be affected in the initial examination.[11]

Updated clinical and genetic data finally enabled us to discover the genetic cause underlying CMT2G. The single family within this category carries the first causal missense mutation in *LRSAM1*, and should thus be reclassified as CMT2P.

Mutations in *LRSAM1* cause autosomal dominant[13,30-32,37-44] or recessive[29,43] CMT2P (for a review, see Palaima et al.[45]). The dominant mutations described so far are associated with a relatively mild, very slowly progressive sensorimotor axonal neuropathy, predominantly or exclusively affecting lower limbs; exceptionally, the clinical picture is dominated by sensory ataxia.[41] Disease onset usually ranges between the second and fourth decade of life, but, as described here and in a family with dominant *LRSAM1* splice site mutation, some patients are asymptomatic.[31] Additionally, three elderly patients carrying an *LRSAM1* frameshift mutation developed Parkinson disease, suggesting a potential role of mutated *LRSAM1* in the degeneration of substantia nigra.[46]

Our study broadened the existing knowledge regarding the phenotypic and genetic spectrum associated with *LRSAM1*.[13] In general, reduced penetrance is rarely observed in CMT subtypes,[35] yet it appears to be a common phenomenon in the context of *LRSAM1*-related neuropathies, as demonstrated by the current and previous research.[31] The finding that some mutation carriers display only pes cavus and minimal electrophysiological features should be carefully considered. As Michael Shy[47] fittingly remarked in the accompanying editorial, "making a genetic diagnosis still depends on careful clinical neurology, even with modern DNA analysis." Furthermore, although pes cavus was a constant manifestation in our patients, we must recognise that there were cases with isolated pes cavus in at-risk subjects who ultimately turned out to be unaffected; thus, they should retrospectively be categorised as idiopathic pes cavus.[26] In other words, "findings such as pes cavus, which were presumed to be diagnostic of CMT, proved not to be so."[47]

Moreover, our findings highlighted the importance of MRI to detect and characterise pathological conditions of the skeletal muscle.[13] In line with previous observations for CMT1A and CMT2A,[27,48,49] the current MRI showed moderate to marked fatty atrophy of foot muscles in all seven subclinical *LRSAM1* mutation carriers. Fatty infiltration of leg muscles was present to a lesser degree, increasing distally throughout the long axis of the muscle belly. As in other dominant axonal CMT phenotypes, fatty atrophy was greater in superficial posterior compartment muscles.[49] The observed predominant fatty infiltration in foot muscles and proximal-to-distal gradient in calf muscles correlated with the dying-back phenomenon found in our previous histological study of the sciatic nerve and its branches (see above). Notably, MRI of a non–mutation carrier showed normal appearance of the calf and foot muscles. Our findings established that patients with minimal clinical symptoms display abnormalities of lower-limb muscles perceptible by MRI, suggesting that muscle MRI could be a useful tool for diagnosing *LRSAM1*-related neuropathies.

Our report illustrated several potential pitfalls of genetic studies.[13] First, thorough examination of an established disease locus (CMT2G on chromosome 12) with state-of-the-art "omics" technologies did not identify the disease-causing mutation. The ultimate gene identification was facilitated by longitudinal clinical follow-up, reassessment of disease statuses, and renewed linkage analysis. Second, the c.2081G *LRSAM1* variant was not covered in the WGS data of the 2 patients studied, so the mutation could only be retrieved after applying an orthogonal sequencing technology (WES). The relatively high raw base-calling error rate and variable performance of NGS platforms is well recognised.[50] Our study highlighted the added value of a dual-platform approach employing complementary NGS protocols[51] to improve variant yield and reduce false-negative calls.

LRSAM1 is a multidomain RING type E3 ubiquitin ligase that covalently ubiquitylates target proteins through its catalytic C-terminal finger domain.[13,45] Figure 11 illustrates the *LRSAM1* domains and location of pathogenic mutations.[45] LRSAM1 has several cellular functions as it

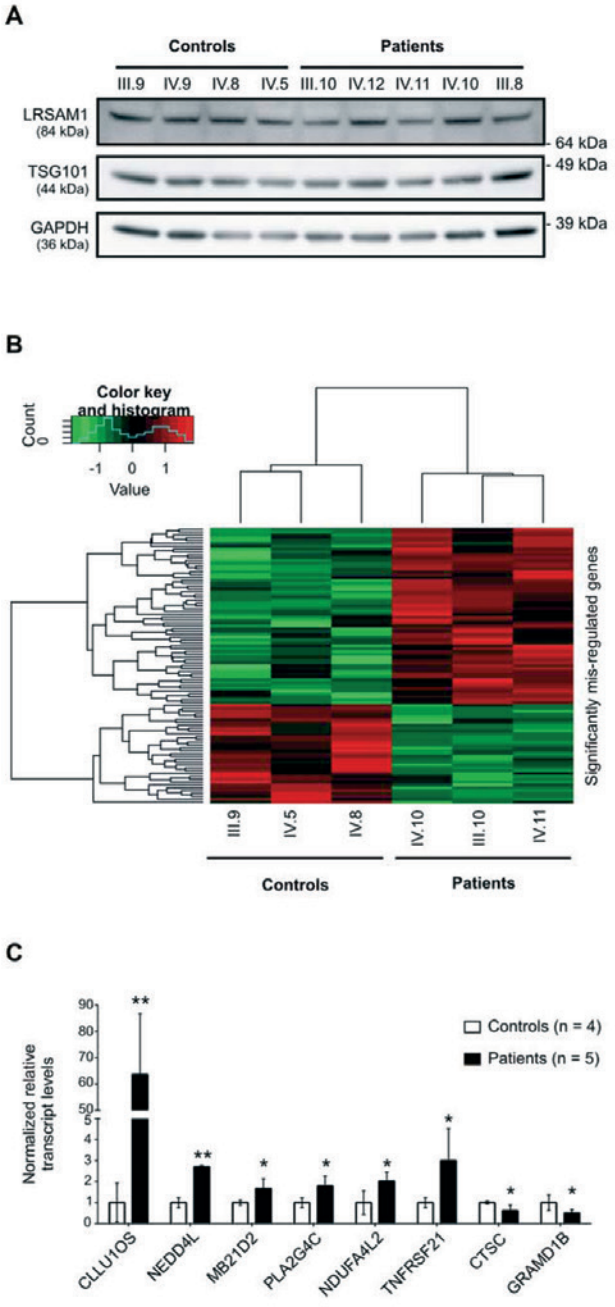

Figure 10. Protein and transcriptional analyses. A) Immunoblot analysis of LRSAM1 and its interactor TSG101 in lysates of lymphoblasts from five patients and four controls. Glyceraldehyde-3-phosphate dehydrogenase (GADPH) was used to demonstrate equal loading. B) Heat map generated from the transcriptome sequencing data reflecting the expression level of the significantly misregulated genes retrieved by DESeq2 (measured in regulated log-transformed read counts) across patient and control samples. C) Real-time quantitative chain reaction analysis showing relative expression levels (normalised to GAPDH, TATA-binding protein, and succinate dehydrogenase complex subunit A) of eight significantly misregulated transcripts in lymphoblasts obtained from five patients compared to four controls. *$P \leq .05$; **$P \leq .01$. Taken from Peeters et al.[13]

modulates protein aggregation, endosomal sorting machinery, and virus egress from the cell, making LRSAM1 interesting not only in protein conformational disorders such as neurodegeneration, but also in immunological and cancer disorders.[52] The only known ubiquitylation target of LRSAM1 is the tumour susceptibility 101 protein (TSG101), which is involved in lysosomal sorting of ubiquitylated cargo.[33] Knockdown of the *LRSAM1* homolog in zebrafish results in abnormal motor neuron development,[30] and knockout of *Lrsam1* in mice sensitised peripheral neurons and axons to other mutations or environmental toxicities.[53] Interestingly, these experimental data correlate well with our histological findings, demonstrating that the pathological framework of CMT2P is a sensorimotor neuronopathy with length-dependent axonal degeneration.

The *LRSAM1* mutations reported at the time of mutation discovery in the AC family (Figure 11[45]) truncate, disrupt, or abolish the protein's catalytic RING zinc finger domain.[13,29-32,45] We reported the first causal mutation in *LRSAM1*, which also targets the RING zinc finger.[13] Synthetic missense mutations in this domain abolish the ubiquitylation function.[33] Likewise, a CMT2P-causing insertion in *LRSAM1* results in increased TSG101 levels in a cellular overexpression model, suggesting that it is not ubiquitylated and degraded.[30] We tested whether the p.Cys694Tyr *LRSAM1* mutation had a similar effect in patients' lymphoblasts. This implies that either the mutation does not abolish the LRSAM1 ubiquitylation function, or the loss of function is compensated by alternative cellular mechanisms. It has been suggested that other ubiquitin ligases can also target excessive amounts of TSG101 for proteasomal degradation to prevent detrimental consequences associated with TSG101 overexpression, such as disrupted endosomal sorting of cellular growth.[54,55] Interestingly, our transcriptomic analysis appears to support this hypothesis. The results in patients' cells showed increased transcription of *NEDD4L*, a gene encoding another E3 ubiquitin ligase targeting TSG101.[13] Therefore, NEDD4L might compensate for loss of LRSAM1 function, which may explain the mild phenotype in LRSAM1 patients.[13]

Additionally, p.Cys694Tyr mutation carriers have increased transcription of *TNFRSF21,* a key regulator of axonal degeneration.[56] Likewise, TNFRSF21 levels are elevated in the spinal cord of patients with amyotrophic lateral sclerosis (ALS)[57] and in the brains of patients with Alzheimer disease,[58] promoting neuronal death through

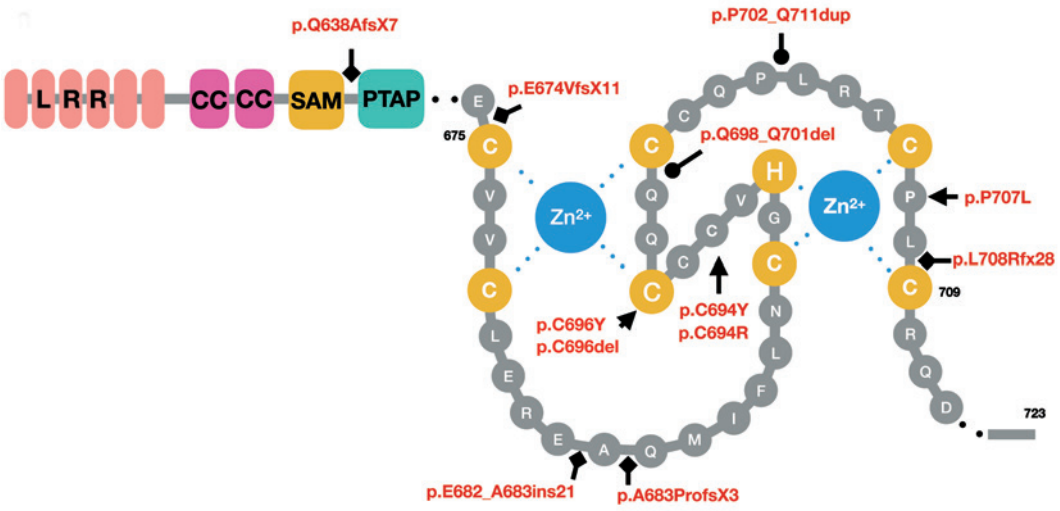

Figure 11. The domains and location of CMT-causing mutations in *LRSAM1*. LRR: leucine-rich repeat; CC: coiled-coil; SAM: sterile alpha motif; PTAP: Pro-Thr-Ala-Pro motif; RING: really interesting gene (expanded view). Frameshift mutations are indicated by square indentations, missense mutations by arrows, and in-frame changes by circle indentations. Critical residues required for the binding of zinc ions (blue) are indicated in yellow. Taken from Palaima et al.[45]

activation of apoptotic caspase signalling pathways. Blocking TNFRSF21 function with an antagonist antibody results in increased motor neuron survival and motor function improvement in ALS mice[57] and protection against Aβ42-induced neurotoxicity in cultured neocortical neurons.[58] It would be interesting to investigate whether this promising therapeutic approach could have a similar neuroprotective effect on CMT2P models and, ultimately, patients. In summary, our transcriptome analysis of CMT2P patients offers new insights into cellular pathways associated with LRSAM1 dysfunction and provides novel targets for further studies.

Conclusions

The identification of the pathogenic mutation in a large CMT2 family with autosomal dominant transmission and incomplete penetrance was preceded by four decades of uninterrupted clinical, electrophysiological, histopathological, and MRI study of the leg and foot muscles to reliably define the clinical phenotype. In 2004, a first linkage analysis led to a misplacement of the responsible gene on chromosome 12q (CMT2G). Better identification of patients among subjects at risk allowed us to redefine the disease-linked region to chromosome 9q and subsequently to identify a novel missense mutation in the *LRSAM1* gene (p.Cys694Tyr). These results are the consequence of the formidable and sustained coordination between Spanish clinicians and Belgian geneticists.

Acknowledgements

We wish to express our deepest gratitude to our colleagues at Marqués de Valdecilla University Hospital, University of Cantabria, University of Antwerp, and VIB for their invaluable help in clinical, neurophysiological, pathological, imaging, and genetic studies, all carried out over four decades of uninterrupted work with the AC family, whose members we also thank for their always prompt collaboration. We also thank Dr José Gazulla for stylistic revision of the manuscript. We would like to pay special tribute to Professor Anita Harding (may she rest in peace), who generously initiated the research addressed herein.

Conflicts of interest

The authors have no conflicts of interest to declare. This study has received no public or private funding.

References

1. Combarros O, Calleja J, Polo JM, Berciano J. Prevalence of hereditary motor and sensory neuropathy in Cantabria. Acta Neurol Scand. 1987;75:9-12.
2. Harding AE, Thomas PK. The clinical features of hereditary motor and sensory neuropathy types I and II. Brain. 1980;103:259-80.
3. Harding AE, Thomas PK. Genetic aspects of hereditary motor and sensory neuropathy (types I and II). J Med Genet. 1980;17:329-36.
4. Harding AE, Thomas PK. Autosomal recessive forms of hereditary motor and sensory neuropathy. J Neurol Neurosurg Psychiatry. 1980;43:669-78.
5. Dyck PJ. Inherited neuronal degeneration and atrophy affecting peripheral motor, sensory and autonomic neurons. In: Dyck PJ, Thomas PK, Lambert EH, Bunge R, eds. Peripheral neuropathy. Philadelphia and London: Saunders; 1984. p. 1600-55.
6. Madrid R, Bradley WG, Davis CJ. The peroneal muscular atrophy syndrome. Clinical, genetic, electrophysiological and nerve biopsy studies. Part 2. Observations on pathological changes in sural nerve biopsies. J Neurol Sci. 1977;32:91-122.
7. Berciano J, García A, Gallardo E, Peeters K, Pelayo-Negro AL, Álvarez-Paradelo S, et al. Intermediate Charcot-Marie-Tooth disease: an electrophysiological reappraisal and systematic review. J Neurol. 2017;264:1655-77.
8. Rossor AM, Polke JM, Houlden H, Reilly MM. Clinical implications of genetic advances in Charcot-Marie-Tooth disease. Nat Rev Neurol. 2013;9:562-71.
9. Pipis M, Rossor AM, Laura M, Reilly MM. Next-generation sequencing in Charcot-Marie-Tooth disease: opportunities and challenges. Nat Rev Neurol. 2019;15:644-56.
10. Parmar JM, Laing NG, Kennerson ML, Ravenscroft G. Genetics of inherited peripheral neuropathies and the next frontier: looking backwards to progress forwards. J Neurol Neurosurg Psychiatry. 2024;95:992-100.
11. Berciano J, Combarros O, Figols J, Calleja J, Cabello A, Silos I, et al. Hereditary motor and sensory neuropathy type II. Clinicopathological study of a family. Brain. 1986;109:897-91.
12. Nelis E, Berciano J, Verpoorten N, Coen K, Dierick I, Van Gerwen V, et al. Autosomal dominant axonal Charcot-Marie-Tooth disease type 2 (CMT2G) maps to chromosome 12q12-q13.3. J Med Genet. 2004;41:193-7.
13. Peeters K, Palaima P, Pelayo-Negro AL, García A, Gallardo E, García-Barredo R, et al. Charcot-Marie-Tooth disease type 2G redefined by a novel mutation in LRSAM1. Ann Neurol. 2016;80:823-33.
14. Tooth HH. The peroneal type of progressive muscular atrophy. London: HK Lewis, 1886.
15. Combarros O, Calleja J, Figols J, Cabello A, Berciano J. Dominantly inherited motor and sensory neuropathy type I. Genetic, clinical, electrophysiological and pathological features in four families. J Neurol Sci. 1983;61:181-91.
16. Middleton-Price HR, Harding AE, Berciano J, Pastor JM, Huson SM, Malcolm S. Absence of linkage of hereditary motor and sensory neuropathy type I to chromosome 1 markers. Genomics. 1989;4:192-7.
17. Middleton-Price HR, Harding AE, Monteiro C, Berciano J, Malcolm S. Linkage of hereditary motor and sensory neuropathy type I to the pericentromeric region of chromosome 17. Am J Hum Genet. 1990;46:92-4.
18. Hallam PJ, Harding AE, Berciano J, Barker DF, Malcolm S. Duplication of part of chromosome 17 is commonly associated with hereditary motor and sensory neuropathy type I (Charcot-Marie-Tooth disease type 1). Ann Neurol. 1992;31:570-2.
19. Raeymaekers P, Timmerman V, Nelis E, De Jonghe P, Hoogendijk JE, Baas F, et al. Duplication in chromosome 17p11.2 in Charcot-Marie-Tooth neuropathy type 1a (CMT1a). The HMSN Collaborative Research Group. Neuromuscul Disord. 1991;1:93-7.
20. Shy ME, Blake J, Krajewski K, Fuerst DR, Laura M, Hahn AF, et al. Reliability and validity of the CMT neuropathy score as a measure of disability. Neurology. 2005;64:1209-14.
21. Shy ME, Chen L, Swan ER, Taube R, Krajewski KM, Herrmann D, et al. Neuropathy progression in Charcot-Marie-Tooth disease type 1A. Neurology. 2008;70:378-83.
22. Berciano J, Combarros O, Calleja J, Polo JM, Leno C. The application of nerve conduction and clinical studies to genetic counseling in hereditary motor and sensory neuropathy type I. Muscle Nerve. 1989;12:302-6.
23. García A, Combarros O, Calleja J, Berciano J. Charcot-Marie-Tooth disease type 1A with 17p duplication in infancy and early childhood: a longitudinal clinical and electrophysiologic study. Neurology. 1998;50:1061-7.
24. Berciano J, García A, Combarros O. Initial semeiology in children with Charcot-Marie-Tooth disease 1A duplication. Muscle Nerve. 2003;27:34-9.
25. Berciano J, Gallardo E, García A, Pelayo-Negro AL, Infante J, Combarros O. New insights into the pathophysiology of pes cavus in Charcot-Marie-Tooth disease type 1A duplication. J Neurol. 2011;258:1594-602.
26. Karakis I, Gregas M, Darras BT, Kang PB, Jones HR. Clinical correlates of Charcot-Marie-Tooth disease in patients with pes cavus deformities. Muscle Nerve. 2013;47:488-92.
27. Gallardo E, García A, Combarros O, Berciano J. Charcot-Marie-Tooth disease type 1A duplication: spectrum of clinical and magnetic resonance imaging features in leg and foot muscles. Brain. 2006;129:426-37.

28. Rossor AM, Tomaselli PJ, Reilly MM. Recent advances in the genetic neuropathies. Curr Opin Neurol. 2016;29:537-48.
29. Guernsey DL, Jiang H, Bedard K, Evans SC, Ferguson M, Matsuoka M, et al. Mutation in the gene encoding ubiquitin ligase LRSAM1 in patients with Charcot-Marie-Tooth disease. PLoS Genet. 2010;6:e1001081.
30. Weterman MA, Sorrentino V, Kasher PR, Jakobs ME, van Engelen BG, Fluiter K, et al. A frameshift mutation in LRSAM1 is responsible for a dominant hereditary polyneuropathy. Hum Mol Genet. 2012;21:358-70.
31. Nicolaou P, Cianchetti C, Minaidou A, Marrosu G, Zamba-Papanicolaou E, Middleton L, et al. A novel LRSAM1 mutation is associated with autosomal dominant axonal Charcot-Marie-Tooth disease. Eur J Hum Genet. 2013;21:190-4.
32. Engeholm M, Sekler J, Schöndorf DC, Arora V, Schittenhelm J, Biskup S, et al. A novel mutation in LRSAM1 causes axonal Charcot-Marie-Tooth disease with dominant inheritance. BMC Neurol. 2014;14:118.
33. Amit I, Yakir L, Katz M, Zwang Y, Marmor MD, Citri A, et al. Tal, a Tsg101-specific E3 ubiquitin ligase, regulates receptor endocytosis and retrovirus budding. Genes Dev. 2004;18:1737-52.
34. Pelayo-Negro AL, Carr AS, Laura M, Skorupinska M, Reilly MM. An observational study of asymmetry in CMT1A. J Neurol Neurosurg Psychiatry. 2015;86:589-90.
35. Berciano J, Baets J, Gallardo E, Zimoń M, García A, López-Laso E, et al. Reduced penetrance in hereditary motor neuropathy caused by TRPV4 Arg269Cys mutation. J Neurol. 2011;258:1413-21.
36. Guiloff RJ, Thomas PK, Contreras M, Armitage S, Schwarz G, Sedgwick EM. Linkage of autosomal dominant type I hereditary motor and sensory neuropathy to the Duffy locus on chromosome 1. J Neurol Neurosurg Psychiatry. 1982;45:669-74.
37. Hu B, Arpag S, Zuchner S, Li J. A novel missense mutation of CMT2P alters transcription machinery. Ann Neurol. 2016;80:834-45.
38. Peddareddygari LR, Oberoi K, Vellore JR, Grewal RP. Factors affecting phenotype variability in a family with CMT2B: gender and LRSAM1 genotype. Case Rep Neurol. 2016;8:120-6.
39. Hakonen JE, Sorrentino V, Avagliano Trezza R, de Wissel MB, van den Berg M, Bleijlevens B, et al. LRSAM1-mediated ubiquitylation is disrupted in axonal Charcot-Marie-Tooth disease 2P. Hum Mol Genet. 2017;26:2034-41.
40. Zhao G, Song J, Yang M, Song X, Liu X. A novel mutation of LRSAM1 in a Chinese family with Charcot-Marie-Tooth disease. J Peripher Nerv Syst. 2018;23:55-9.
41. Peretti A, Perie M, Vincent D, Bouhour F, Dieterich K, Mallaret M, et al. LRSAM1 variants and founder effect in French families with ataxic form of Charcot-Marie-Tooth type 2. Eur J Hum Genet. 2019;27:1406-18.
42. Mortreux J, Bacquet J, Boyer A, Alazard E, Bellance R, Giguet-Valard AG, et al. Identification of novel pathogenic copy number variations in Charcot-Marie-Tooth disease. J Hum Genet. 2020;65:313-23.
43. Reilich P, Schlotter B, Montagnese F, Jordan B, Stock F, Schäff-Vogelsang M, et al. Location matters - Genotype-phenotype correlation in LRSAM1 mutations associated with rare Charcot-Marie-Tooth neuropathy CMT2P. Neuromuscul Disord. 2021;31:123-33.
44. Milella G, Amati A, Lastella P, Zanfardino P, Petruzzella V, Zoccolella S. A novel mutation in the LRSAM1 gene in a family with early onset autosomal dominant Charcot-Marie-Tooth type 2P. Clin Neurol Neurosurg. 2024;237:108158.
45. Palaima P, Berciano J, Peeters K, Jordanova A. LRSAM1 and the RING domain: Charcot-Marie-Tooth disease and beyond. Orphanet J Rare Dis. 2021;16:74.
46. Aerts MB, Weterman MA, Quadri M, Schelhaas HJ, Bloem BR, Esselink RA, et al. A LRSAM1 mutation links Charcot-Marie-Tooth type 2 to Parkinson's disease. Ann Clin Transl Neurol. 2015;3:146-9.
47. Shy M. LRSAM1 lessons. Ann Neurol. 2016;80:821-2.
48. Berciano J, Gallardo E, García A, Infante J, Mateo I, Combarros O. Charcot-Marie-Tooth disease type 1A duplication with severe paresis of the proximal lower limb muscles: a long-term follow-up study. J Neurol Neurosurg Psychiatry. 2006;77:1169-76.
49. Chung KW, Suh BC, Shy ME, Cho SY, Yoo JH, et al. Different clinical and magnetic resonance imaging features between Charcot-Marie-Tooth disease type 1A and 2A. Neuromuscul Disord. 2008;18:610-8.
50. Lelieveld SH, Spielmann M, Mundlos S, Veltman JA, Gilissen C. Comparison of exome and genome sequencing technologies for the complete capture of protein-coding regions. Hum Mutat. 2015;36:815-22.
51. Chennagiri N, White EJ, Frieden A, Lopez E, Lieber DS, Nikiforov A, et al. Orthogonal NGS for high throughput clinical diagnostics. Sci Rep. 2016;6:24650.
52. Mishra R, Upadhyay A, Prajapati VK, Dhiman R, Poluri KM, Jana NR, et al. LRSAM1 E3 ubiquitin ligase: molecular neurobiological perspectives linked with brain diseases. Cell Mol Life Sci. 2019;76:2093-110.
53. Bogdanik LP, Sleigh JN, Tian C, Samuels ME, Bedard K, Seburn KL, et al. Loss of the E3 ubiquitin ligase LRSAM1 sensitizes peripheral axons to degeneration in a mouse model of Charcot-Marie-Tooth disease. Dis Model Mech. 2013;6:780-92.

54. McDonald B, Martin-Serrano J. Regulation of Tsg101 expression by the steadiness box: a role of Tsg101-associated ligase. Mol Biol Cell. 2008;19:754-63.
55. Chung HY, Morita E, von Schwedler U, Müller B, Kräusslich HG, Sundquist WI. NEDD4L overexpression rescues the release and infectivity of human immunodeficiency virus type 1 constructs lacking PTAP and YPXL late domains. J Virol. 2008;82:4884-97.
56. Wang Y, Zhao D, Pan B, Song Z, Shah SZA, Yin X, et al. Death receptor 6 and caspase-6 regulate prion peptide-induced axonal degeneration in rat spinal neurons. J Mol Neurosci. 2015;56:966-76.
57. Huang G, Lee X, Bian Y, Shao Z, Sheng G, Pepinsky RB, et al. Death receptor 6 (DR6) antagonist antibody is neuroprotective in the mouse SOD1G93A model of amyotrophic lateral sclerosis. Cell Death Dis. 2013;4:e841.
58. Hu Y, Lee X, Shao Z, Apicco D, Huang G, Gong BJ, et al. A DR6/p75(NTR) complex is responsible for beta-amyloid-induced cortical neuron death. Cell Death Dis. 2013;4:e579.